A hypermorphic IκBα mutation is associated with autosomal dominant anhidrotic ectodermal dysplasia and T cell immunodeficiency

See the related Commentary beginning on page 983.

Gilles Courtois,[1] Asma Smahi,[2] Janine Reichenbach,[3] Rainer Döffinger,[3] Caterina Cancrini,[4] Marion Bonnet,[3] Anne Puel,[3] Christine Chable-Bessia,[1] Shoji Yamaoka,[5] Jacqueline Feinberg,[3] Sophie Dupuis-Girod,[6] Christine Bodemer,[7] Susanna Livadiotti,[4] Francesco Novelli,[3] Paolo Rossi,[4] Alain Fischer,[8,9] Alain Israël,[1] Arnold Munnich,[2] Françoise Le Deist,[8] and Jean-Laurent Casanova[3,9]

[1]Unité de Biologie Moléculaire de l'Expression Génique, Centre National de la Recherche Scientifique (CNRS) URA 2582, Institut Pasteur,
[2]Unité de Recherches sur les Handicaps Génétiques de l'Enfant, Institut National de la Santé et de la Recherche Médicale (INSERM) U393, Hôpital Necker-Enfants Malades, and
[3] Laboratoire de Génétique Humaine des Maladies Infectieuses, Université de Paris René Descartes INSERM U550, Faculté de Médecine Necker-Enfants Malades, Paris, France
[4]Division of Immunology and Infectious Disease, Children's Hospital Bambino Gesù, University of Rome Tor Vergata, Rome, Italy
[5]Department of Molecular Virology, Graduate School of Medicine, Tokyo Medical and Dental University, Tokyo, Japan
[6]Unité d'Immunologie et d'Hématologie Pédiatriques, Hôpital Debrousse, Lyon, France
[7]Service de Dermatologie,
[8]Développement Normal et Pathologique du Système Immunitaire, INSERM U429, and
[9]Unité d'Immunologie et d'Hématologie Pédiatriques, Hôpital Necker-Enfants Malades, Paris, France

X-linked anhidrotic ectodermal dysplasia with immunodeficiency (XL-EDA-ID) is caused by hypomorphic mutations in the gene encoding NEMO/IKKγ, the regulatory subunit of the IκB kinase (IKK) complex. IKK normally phosphorylates the IκB-inhibitors of NF-κB at specific serine residues, thereby promoting their ubiquitination and degradation by the proteasome. This allows NF-κB complexes to translocate into the nucleus where they activate their target genes. Here, we describe an autosomal-dominant (AD) form of EDA-ID associated with a heterozygous missense mutation at serine 32 of IκBα. This mutation is gain-of-function, as it enhances the inhibitory capacity of IκBα by preventing its phosphorylation and degradation, and results in impaired NF-κB activation. The developmental, immunologic, and infectious phenotypes associated with hypomorphic *NEMO* and hypermorphic *IKBA* mutations largely overlap and include EDA, impaired cellular responses to ligands of TIR (TLR-ligands, IL-1β, and IL-18), and TNFR (TNF-α, LTα1/β2, and CD154) superfamily members and severe bacterial diseases. However, AD-EDA-ID but not XL-EDA-ID is associated with a severe and unique T cell immunodeficiency. Despite a marked blood lymphocytosis, there are no detectable memory T cells in vivo, and naive T cells do not respond to CD3-TCR activation in vitro. Our report highlights both the diversity of genotypes associated with EDA-ID and the diversity of immunologic phenotypes associated with mutations in different components of the NF-κB signaling pathway.

J. Clin. Invest. **112**:1108–1115 (2003). doi:10.1172/JCI200318714.

Introduction

Patients with anhidrotic ectodermal dysplasia with immunodeficiency (EDA-ID) present with impaired development of skin appendices, resulting in sparse hair, conical teeth, and anhidrosis/hypohidrosis. Host defense is also impaired, resulting principally in multiple and severe bacterial diseases (1). X-linked EDA-ID (XL-EDA-ID) is caused by hypomorphic mutations in the gene encoding NEMO/IKKγ, the regulatory subunit of the IκB kinase (IKK) complex (1–8). IKK nor-

Received for publication April 22, 2003, and accepted in revised form August 12, 2003.

Address correspondence to: Jean-Laurent Casanova, Laboratoire de Génétique Humaine des Maladies Infectieuses, Université de Paris René Descartes-INSERM U550, Faculté de Médecine Necker-Enfants Malades, 156 rue de Vaugirard, 75015 Paris, France. Phone: 33-1-40-61-53-81; Fax: 33-1-40-61-56-88; E-mail: casanova@necker.fr.
Rainer Döffinger's present address is: Department of Clinical Biochemistry and Immunology, Addenbrookes Hospital, Cambridge, United Kingdom.
Francesco Novelli's present address is: Centro Oncologico Ematologico Subalpino, Centro Ricerche Medicina Sperimentale, Ospedale San Giovanni Battista, Torino, Italy.
Asma Smahi, Janine Reichenbach, and Rainer Döffinger contributed equally to this work.
Conflict of interest: The authors have declared that no conflict of interest exists.
Nonstandard abbreviations used: anhidrotic ectodermal dysplasia with immunodeficiency (EDA-ID); X-linked (XL); inhibitor of NF-κB (IκB); IκB kinase (IKK); autosomal-dominant (AD); osteopetrosis, lymphedema, and EDA-ID (OL-EDA-ID); phytohemagglutinin (PHA); incontinentia pigmenti (IP); phycoerythrin (PE).

mally phosphorylates the IκB inhibitors of NF-κB at specific serine residues, thereby promoting their ubiquitination and degradation by the proteasome. This in turn allows NF-κB complexes to translocate into the nucleus where they activate their target genes (9). In patients with XL-EDA-ID, impaired immunity results at least from impaired NEMO-dependent NF-κB activation by members of the Toll and interleukin-1 receptors (TIR) (Toll-like receptors [TLR], IL-1R, and IL-18R) and tumor necrosis factor receptors (TNFR) (TNF-αR and CD40) superfamilies (3, 4), and EDA results from impaired NF-κB activation by the TNFR superfamily member EDA-R (3).

The routine immunologic workup of XL-EDA-ID patients shows a lack of specific serum antibodies against polysaccharides in all patients (1, 3), low levels of serum IgG and/or IgA levels in many patients (3, 4), and impaired NK activity in some patients (8). Other current diagnostic laboratory assays are generally normal. In particular, these patients have normal numbers of naive and memory T cells, which respond well to protein antigens. We herein describe the investigation of a child with EDA-ID and a severe T cell immunodeficiency. Antibody- and antigen-induced activation of T cells through the CD3-TCR complex were abolished in vitro and no memory T cells were detectable in vivo, despite a marked lymphocytosis. We show that the patient had a novel, autosomal dominant form of EDA-ID caused by a heterozygous gain-of-function mutation of IκBα. This mutation enhances the inhibitory capacity of IκBα by preventing its phosphorylation and degradation, thereby impairing NF-κB activation in heterozygous cells.

Methods

Case report. The clinical features will be described in detail elsewhere (S. Dupuis-Girod and C. Cancrini, unpublished observations). The boy was born to unrelated RelA parents, and since 2 months of age he has had chronic diarrhea, recurrent bronchopneumonitis, hepatosplenomegaly, and failure to thrive (patient P). Several Gram-positive and Gram-negative pyogenic bacteria were involved, requiring parenteral antibiotics and nutrition. When the child received bone marrow transplantation at 1 year of age, there were high numbers of peripheral blood leukocytes (35,000–45,000/mm^3) with polyclonal lymphocytosis (20,000–30,000/mm^3). The B (CD19), NK (CD16/CD56), and T (CD3, CD3/CD4, CD3/CD8, and CD3/TCRα/β) lymphocyte subsets were normally distributed (Table 1). Serum IgM levels reached 5 g/l, whereas IgG and IgA levels remained below 1 g/l and 0.1 g/l, respectively. No serum antibodies specific for recall antigens were detected. The NK activity was normal. Interestingly, there were no detectable γ/δ T cells and all α/β T cells had the naive CD45RA phenotype, with a lack of detectable CD45RO memory T cells. There was also a complete lack of proliferation in response to CD3-specific antibodies (Table 2). The response to CD3 was, however, restored after stimulation with recombinant IL-2 or CD28-specific antibody. Proliferation in response to lectins (e.g., phytohemagglutinin [PHA], pokeweed mitogen, and Concanavalin A), allogeneic cells, SEB, and PMA-ionomycin was normal. After natural exposure or vaccination, the patient's T cells failed to respond to all recall antigens tested, including tetanus toxoid, poliovirus, tuberculin, and candidin (Table 2; not shown). All other patients with XL-EDA-ID tested, including a patient (patient X-EDA-ID) with the most severe form of XL-EDA-ID (osteopetrosis, lymphedema, and EDA-ID [OL-EDA-ID]), had normal numbers of memory T cells, which proliferated well in response to CD3 and antigens (Tables 1 and 2). A diagnosis of EDA-ID was made around 3 years of age, on the basis of a dry, rough skin, moderately sparse scalp hair, and conical teeth. The child is now 7 years old and there are no other overt developmental defects. His first-degree relatives are healthy, with no signs of EDA-ID or incontinentia pigmenti (IP). The current study has been performed in compliance with the local institute's human subject and informed consent guidelines. Local ethical committee's approval was obtained before the study.

Molecular genetics. RNA was isolated from patient's fibroblasts using the Trizol method, and cDNA was prepared by random-primed reverse transcription using the Gene Amp RNA PCR Core kit (PerkinElmer Applied Biosystems, Courtaboeuf, France). Specific primers (see supplementary information at www.jci.org/cgi/content/full/112/7/1108/DC1) were used to amplify the IκBα cDNA. Genomic DNA was prepared from patient's fibroblasts by standard phenol/chloroform extraction and individual exons of the *IKBA* gene were amplified by PCR using specific primers (see supplementary information). Both the IκBα cDNA and *IKBA* exons were sequenced with the Big Dye Terminator

Table 1
Lymphocytes subsets in the blood

	Patient	X-EDA-ID	Normal values
Lymphocytes (/mm^3)	18,000	3,400	2,700–5,400
T lymphocytes (%)			
CD3	71	63	58–67
CD4	53	40	38–50
CD8	15	20	18–25
CD45RA/CD4	92	76	66–88
CD45RO/CD4	1	17	17–39
CD45RA/CD8	97	87	70–90
CD45RO/CD8	0	13	15–35
TCRα/β	99	NT	90–97
TCRγ/δ	0	NT	3–10
B lymphocytes (%)			
CD19	23	32	19–31
NK cells (%)			
CD16 and CD56	10	3	3–12

Values are expressed in percentage of lymphocytes, with the exception of CD45RA or CD45RO/CD4 or CD8, which indicate the percentage of CD45RA or CD45RO among CD4 or CD8 T cells. Patients were analyzed at 9 months of age. NT, not tested.

Table 2
T cell proliferation in vitro

Stimulus	Patient	X-EDA-ID	Normal values
Mitogens (d3)			
Medium	2	1.6	<2
SEB	250	NT	>50
PMA-ionomycin	230	NT	>50
PHA	204	96	>50
OKT3	2	206	>20
OKT3 + IL-2	63	NT	>30
OKT3 + CD28	103	NT	>30
Antigens (d6)			
Medium	1	1	<2
Candidin	1	9	>10
TT	1	26	>10
Allogeneic cells	31	NT	37

PBMCs were purified by Ficoll and T cell proliferation was determined at day 3 (d3) or day 6 (d6) by radio-labeled thymidine incorporation. Values are expressed in 10^3 cpm. *Staphylococcus enterotoxin* B (SEB) was used at 10 μg/ml; phytohemagglutinin (PHA) at final dilution 1/700; anti-CD28 at 10 μg/ml; PMA and ionomycin at 10^{-8} and 10^{-6} M, respectively; OKT3 at 50 ng/ml; IL-2 at 20 IU/ml; candidin and tetanus toxoid (TT) at 50 μg/ml and final dilution 1/250, respectively; allogeneic cells were added at 1:1 ratio. In the latter case, the normal value indicated was measured in the same experiment when two controls were used for allogeneic stimulation.

cycle sequencing kit (PerkinElmer Applied Biosystems).

Molecular biology. Western blot analysis, electrophoretic mobility shift assay (EMSA), luciferase assays, and ELISAs were carried out as previously described using skin-derived primary or SV40-transformed fibroblasts (3, 10, 11). The recombinant cytokines used were the same used to stimulate PBMCs, with the exception of 50 ng/ml lymphotoxin α1/β2 (LTα1/β2) (R&D, Abingdon, United Kingdom). Serine 32 (Ser32) phosphorylation was analyzed using an anti-phospho-IκBα antibody from Cell Signaling (Beverly, Massachusetts, USA). IFN-γ, TNF-α, and IL-6 secretion were measured by ELISA (TEBU/CLB; Sanquin, Amsterdam, The Netherlands; R&D). The IKK assay was performed as previously described (12). Mutation Ser32Ile was introduced into human IκBα cDNA (13) using standard PCR procedures.

PBMC activation. PBMCs were isolated from fresh heparinized blood by separation with Lymphoprep (Nicomed Pharma, Oslo, Norway). PBMC were stimulated with 50 ng/ml IL-1β (R&D), 50 ng/ml IL-12 (R&D), 50 ng/ml IL-18 (R&D), 5×10^3 IU/ml IFN-γ (Boehringer Ingelheim), or LPS (*Escherichia coli* serotype 055:55, Sigma-Aldrich, St Louis, Missouri, USA) for 2 days, with PHA (Difco, Detroit, Michigan, USA; final dilution 1/700) for 3 days, with 50 ng/ml anti-CD3 (OKT3, Ortho Diagnostic, Rajitan, New Jersey, USA), 10 μg/ml *Staphylococcus enterotoxin* B (Sigma-Aldrich), 10^{-8} M PMA (Sigma-Aldrich), 10^{-6} M ionomycin (Calbiochem, San Diego, California, USA), 10 μg/ml anti-CD28 (CD28.2, Immunotech, Marseille, France), 20 UI/ml IL-2 (PeproTech Inc., London, United Kingdom) for 4 days, with tetanus toxoid (Pasteur Merieux, Lyon, France; final dilution, 1/250), 50 μg/ml *Candida albicans* somatic antigen (Biorad, Marne la coquette, France), or irradiated allogeneic cells (ratio 1:1) for 6 days. Results are expressed as mean incorporation of [^{3}H]thymidine for the last 18 hours of the culture.

Immunofluorescence. The following mAbs were used in immunofluorescence studies: anti-CD3: Leu 4 (IgG2a, Becton Dickinson, San Diego, California, USA); anti-CD4: Leu 3a (IgG1, Becton Dickinson); anti-CD8: Leu 2a (IgG1, Becton Dickinson); anti-CD19: J4 119 (IgG1, Immunotech); anti-CD16: 3G8 (IgG1, Immunotech); anti-CD56: MY31 (IgG1, Becton Dickinson); anti-TCR α/β: BMA031 (IgG1, Immunotech); anti-TCR γ/δ: IMMU 515 (IgG1, Immunotech); anti-CD45RO: UCHL1 (IgG2a, Immunotech); anti-CD45RA: 2H4 (IgG1, Coulter Clone, Margency, France); anti-HLA DR: L243 (IgG2a, Becton Dickinson); and anti-CD25: 2A3 (IgG1, Becton Dickinson). Fluorescence staining was performed with phycoerythrin (PE) or FITC-conjugated mAbs on whole blood. Cells were analyzed on a FACScan flow cytometer (Becton Dickinson, Franklin Lakes, New Jersey, USA).

T cell analysis. T cell blasts were generated by stimulating frozen PBMC with 5 μg/ml PHA (Sigma-Aldrich), 50 U/ml rh-IL-2 (PeproTech, Inc.), and allogeneic irradiated PBMCs (5×10^5 allogeneic irradiated PBMCs per 1×10^6 PBMCs). FACScan analysis showed that all T cell blasts had normally acquired the CD45RO phenotype on day 10 after stimulation. On day 10, the cells were washed, adjusted to a concentration of 250,000 cells/ml, and plated in triplicate on a 96-well culture plate that had been coated with the following antibodies overnight: 0.1 μg/ml anti-CD3 (BD Biosciences Pharmingen, Le Pont de Claix, France) alone or in combination with 5 μg/ml soluble anti-CD28 (BD Pharmingen) or 2.5 μg/ml PHA (Sigma-Aldrich). Supernatants were taken at 48 hours and IFN-γ production was measured by commercial ELISA kits (Pelikine IFN-γ from CLB, Amsterdam, The Netherlands). Cells were then labeled with [^{3}H]thymidine for 16 hours, and cell proliferation was determined by liquid scintillation counting.

Results and Discussion

As the patient under study and those with XL-EDA-ID had different, yet related, clinical and immunologic phenotypes (case report section; Tables 1 and 2), we tested the patient's NF-κB signaling pathway and analyzed the response of primary fibroblasts to TNF-α and IL-1β by EMSA. The amount of nuclear DNA-binding p50/p50 and p50/RelA dimers was reduced in TNF-α–treated patient P-derived cells compared with a healthy control (Figure 1a and data not shown). The defect seen in patient P fibroblasts was not due to reduced expression of p50 or RelA in the cytoplasm (Figure 1b). In the NEMO-deficient child with OL-EDA-ID (X-EDA-ID), p50/RelA, but not p50/p50, was affected. In response to both TNF-α and IL-1β, IL-6 secretion by fibroblasts was strongly and equally impaired in patients P and X-EDA-ID when compared with a healthy control (Figure 1c). Interestingly, IL-6 secretion in response to LTα1/β2 was also impaired in patients

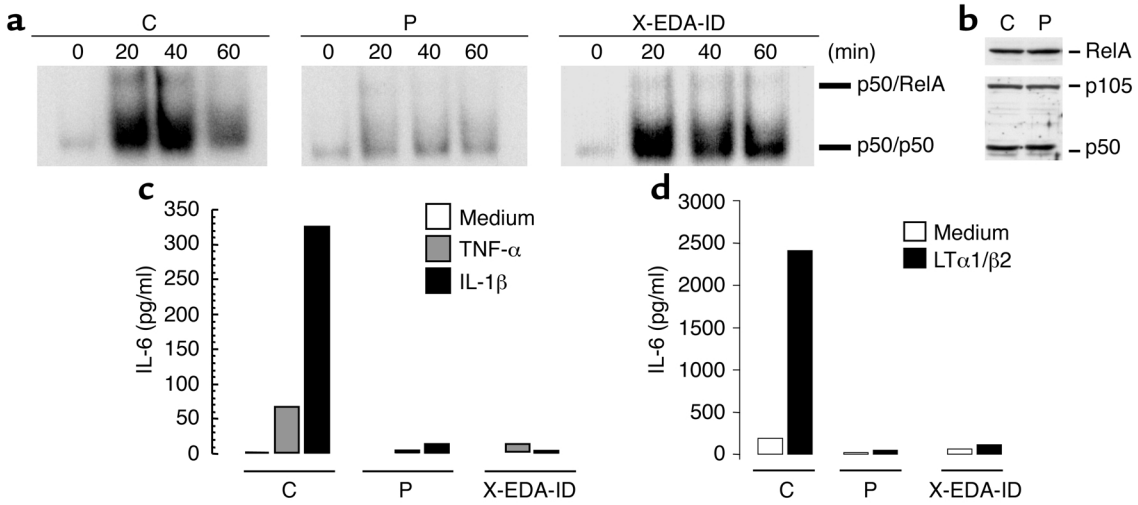

Figure 1
Defective NF-κB activation in patient's fibroblasts. (**a**) EMSA after exposure to 10 ng/ml TNF-α. The composition of the retarded species is indicated on the right and was determined as described in Smahi et al. (10). C, control fibroblasts; P, fibroblasts from patient under study; X-EDA-ID, patient with OL-EDA-ID fibroblasts. (**b**) Western blot analysis of cytoplasmic RelA, p105, and p50.(**c**) Analysis of IL-6 synthesis by primary fibroblasts from patients and a healthy control. Cells were treated overnight with 10 ng/ml of TNF-α or IL-1β, and IL-6 secretion was measured in the supernatant using ELISA. Results from one representative experiment are shown. (**d**) Analysis of IL-6 synthesis by SV-40-transformed fibroblasts from patients and a healthy control. Cells were treated for 24 hours with 50 ng/ml of LTα1/β2, and IL-6 secretion was measured in the supernatant using ELISA. Results from one representative experiment are shown.

P and X-EDA-ID (Figure 1d). This indicates that the impaired DNA-binding activity had a functional impact on the transcription of target genes.

To further dissect the NF-κB pathway in our patient, we performed an IKK assay after immunoprecipitation with anti-NEMO (Figure 2a). IKK activation was normal in our patient P, both in terms of kinetics and efficiency, unlike in the child with XL-EDA-ID tested. Moreover, no mutations were found in the coding region of the XL-EDA-ID disease-causing gene, *NEMO* (not shown), the product of which was detected by Western blotting in fibroblasts (Figure 2b). Finally, as *Ikk2* and *Nemo* KO mice share several phenotypic features (14–19), we analyzed the *IKK2* gene. We found that the sequence of this gene (not shown) and expression of its product (Figure 2b) were normal in the patient. Taken together, these studies indicated that our patient exhibits impaired NF-κB activation due to a molecular defect downstream of the IKK complex, unlike patients with XL-EDA-ID who bear mutations in *NEMO,* resulting in impaired IKK activity.

We thus analyzed IκBα degradation in response to TNF-α by Western blotting (Figure 2a). As previously shown, the degradation of IκBα was reduced, but not

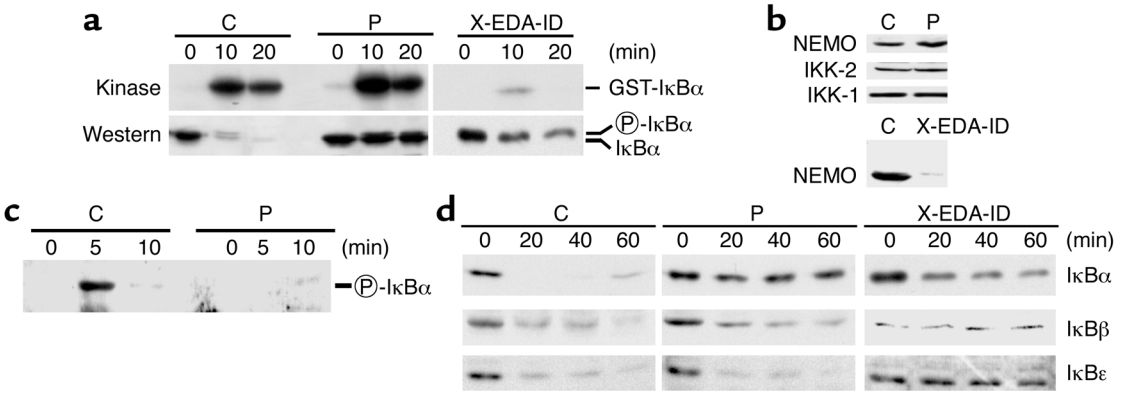

Figure 2
Specific defect of IκBα degradation in patient's fibroblasts treated with TNF-α (**a**) IKK kinase assay and Western blot analysis of IκBα degradation. Phosphorylated IκBα exhibits a retarded migration and is indicated on the right. GST-IκBα, a fusion between gluthatione-S-Transferase and the first 72 amino acids of IκBα, was used as a substrate for IKK. GST, gluthatione-S-transferase. (**b**) Western blot analysis of IKK subunits in fibroblasts from a healthy control, NEMO-mutated patient X-EDA-ID and IκBα-mutated patient P. (**c**) Western blot analysis of IκBα Ser32 phosphorylation after TNF-α stimulation. Circled P, phosphorylated. (**d**) Time course analysis of TNF-induced IκBα, IκBβ, and IκBε degradation, as detected by Western blot. Results from one representative experiment are shown.

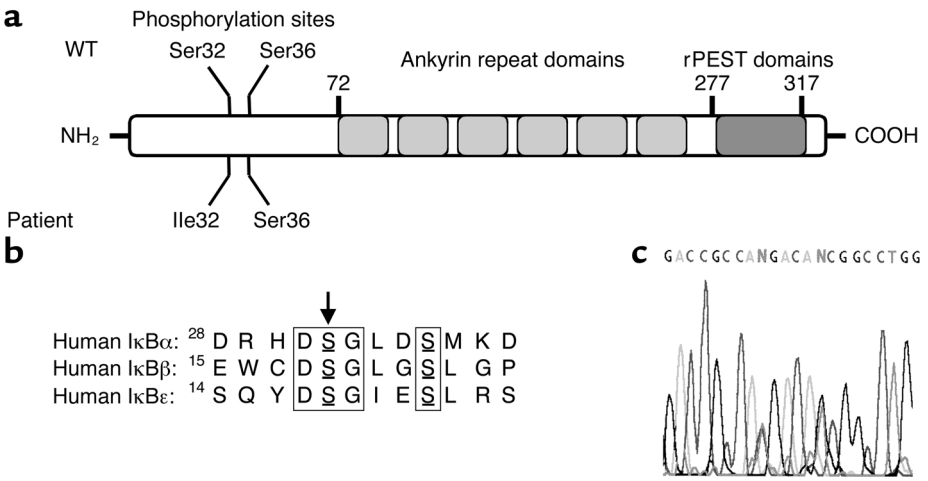

Figure 3
Sequence of the *IKBA* gene in the patient and his relatives. (**a**) Schematic representation of IκBα. The various functional/structural domains of the protein are shown. NH2, N-terminal; rPEST, repeated peptidic sequence rich in proline, glutamic acide, serine, and threonine (PEST); Ile, isoleucine. (**b**) Phosphoacceptor sites of IκB molecules and location of the patient's mutation S32I. The two conserved serine residues that are phosphorylated by IKK in IκBα, IκBβ, and IκBε are boxed. Mutated Ser32 of patient P is indicated by an arrow. (**c**) Automated sequencing profile of genomic DNA showing the heterozygous C/T polymorphism at position 89 and the heterozygous G/T (S32I) disease-causing mutation at position 94 in our patient. The two heterozygous positions from left (position 89) to right (position 94) appear as N nucleotides.

abolished, in fibroblasts from the child X-EDA-ID with OL-EDA-ID carrying a hypomorphic mutation in *NEMO* (3). Almost no decrease in the level of IκBα was seen with our patient P fibroblasts, whereas IκBα almost completely disappeared in fibroblasts from a healthy control. A similar observation was made in response to IL-1β (not shown). These data further suggest that our patient and patients with XL-EDA-ID have distinct genetic disorders in the NF-κB pathway. Importantly, the shifted form of IκBα, which results from its phosphorylation by IKK, did not accumulate in patient P, suggesting that the defect affected the phosphorylation of IκBα. To confirm this hypothesis we analyzed IκBα phosphorylation in TNF-stimulated patient P cells using an antibody specifically recognizing phospho-Ser32. Phosphorylation at this site appeared strongly reduced, representing less than 10% of Ser32 phosphorylation observed in WT cells (Figure 2c).

We then analyzed the fate of the other two inhibitors of NF-κB (IκBβ and IκBε), which are also phosphorylated by IKK in response to TNF-α. In fibroblasts from patient X-EDA-ID, IκBα degradation was impaired but not abolished, whereas that of both IκBβ and IκBε was abolished (Figure 2d). In contrast, the degradation of both IκBβ and IκBε inhibitors was normal in patient P, suggesting that IκBα degradation is specifically impaired and that there is a defect in the *IKBA* gene encoding IκBα. We first sequenced IκBα cDNA by use of three primer pairs covering the entire coding region. We found a G to T substitution at position 94 (not shown). This substitution results in a heterozygous serine to isoleucine substitution at position 32 of the protein (designated S32I) (Figure 3a). Ser32 is a key phospho-acceptor site of IκBα, and is conserved in the other two IκB proteins (Figure 3b). This mutation was confirmed by sequencing the *IKBA* gene (Figure 3c). Interestingly, it abolishes an MspA1 restriction site, a feature that allowed us to quickly demonstrate its absence in 100 healthy white controls (200 chromosomes). The S32I mutation was not found in the parents or in healthy siblings, suggesting that the mutational event occurred de novo in one of the parental germlines. We also detected a heterozygous silent polymorphism in the same region (C to T at position 89) (data not shown). No other mutations were found in the remaining *IKBA* exons.

Previous studies have unambiguously established that mutations of IκBα at Ser32 are gain-of-function, as they

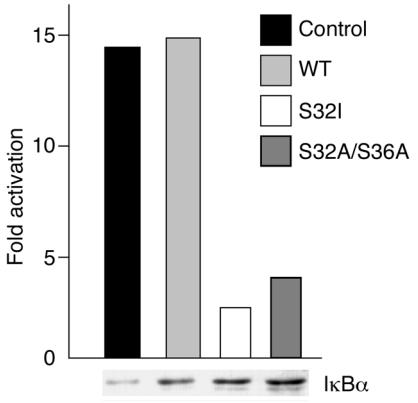

Figure 4
Dominant effect of the S32I *IKBA* mutation on NF-κB activation. HEK 293T cells were transfected with Igκ-luc, a reporter plasmid for NF-κB, and either an empty expression vector (control) or an expression vector encoding WT IκBα (WT), the S32I mutant or the S32A/S36A double mutant. Twenty-four hours later, the cells were stimulated with TNF-α. The relative expression of IκBα molecules is shown at the bottom, as detected by Western blotting.

enhance the NF-κB–inhibitory function of IκBα by preventing its degradation (13, 20–23). This is explained by the fact that IκBα must be phosphorylated on both Ser32 and Ser36 to be recognized by the E3 complex that tags it with ubiquitin for proteasome-dependent clearance. The expression of IκBα molecules with a missense mutation at Ser32 was previously used as an efficient way of blocking NF-κB signaling in WT cells (13, 20–23). Although mutation S32I had not specifically been used in theses studies, they strongly suggested that the S32I allele was dominant. Moreover, we showed that the S32I and WT *IKBA* mRNAs were equally expressed in our patient's cells, as detected by direct sequencing of RT-PCR products (not shown). To unambiguously document the dominant feature of the S32I mutation, we further showed that the S32I *IKBA* allele exerts a strong inhibitory effect on NF-κB activation on transfection in 293T cells stimulated by TNF-α (Figure 4a).

Our studies have shown that the S32I allele is detrimental in S32I/WT heterozygous cells, not only in terms of NF-κB activation (Figure 1a) but also in terms of IκBα degradation (Figure 2a). Interestingly, less than 10% of IκBα was phosphorylated and degraded in WT/S32I *IKBA* fibroblasts on TNF-α stimulation (Figure 2a), although about 50% degradation would be expected in heterozygous cells. The strong dominant effect of the S32I allele may be explained by our previous analysis of IP, in which IKK/NF-κB activation is abolished as a result of loss-of-function *NEMO* mutations (10). The amount of IκBα was increased in resting IP fibroblasts, suggesting that IKK directly controls the steady-state level of IκBα. It is therefore tempting to speculate that S32I IκBα molecules accumulate and represent the vast majority of IκBα species in our patient. In any case, our study demonstrates that an autosomal dominant form of EDA-ID can be caused by hypermorphic mutations in *IKBA*.

Having identified the molecular basis of EDA-ID in our patient, we attempted to characterize the immunologic consequences of the S32I IκBα dominant mutation. The hyper-IgM phenotype of the patient strongly suggested that his B cell response to CD40 stimulation was abnormal in terms of IgE secretion, proliferation or both. B cells from the previously reported child with OL-EDA-ID and hyper-IgM were able to switch but not to proliferate after CD40 stimulation (3). The hyper-IgM syndrome was, however, not a consistent feature of NEMO-deficient patients with EDA-ID (3, 4). Blood

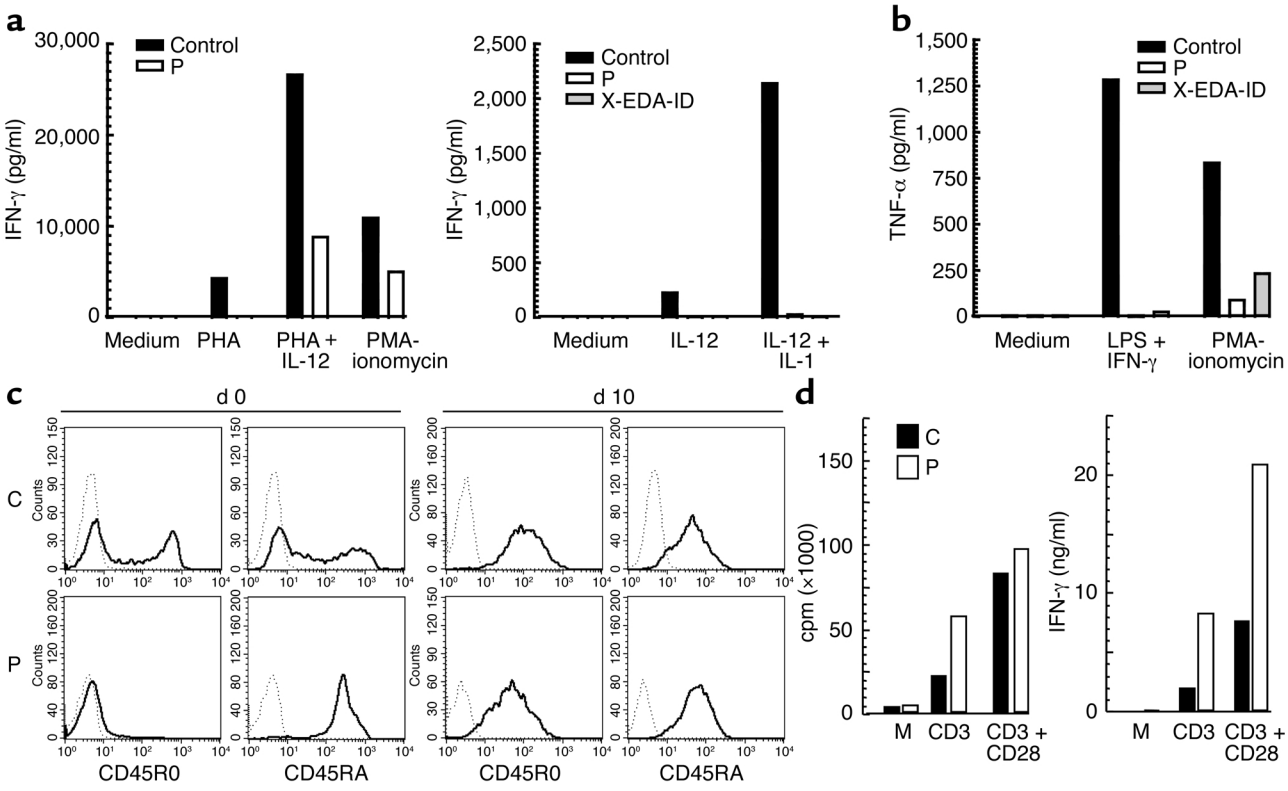

Figure 5

PBMC and T cell analysis. (**a**) Peripheral blood cells from patient P, a healthy control, and patient X-EDA-ID with OL-EDA-ID were stimulated by PHA, PMA-ionomycin, IL-12, IL-12 + IL-1β, or PHA, and IFN-γ secretion was measured by ELISA. Results from one representative experiment are shown. (**b**) Peripheral blood cells were stimulated by PMA-ionomycin or LPS + IFN-γ, and TNF-α secretion was measured by ELISA. Results from one representative experiment are shown. (**c**) CD45RA and CD45RO expression on control (C) and patient (P) T cells at day 0 and day 10 of PHA + IL-2 stimulation in vitro, as detected by flow cytometry. (**d**) T cell proliferation (left) after 64 hours of stimulation with anti-CD3 alone, or anti-CD3 in combination with anti-CD28. Production of IFN-γ (right) in culture supernatants after 48 hours of stimulation with anti-CD3 alone or in combination with anti-CD28. Results from one representative experiment are shown. Data are normalized for 10^6 cells.

IFN-γ production in response to IL-12 plus IL-1β, and to a lesser extent in response to IL-12 plus PHA, was impaired in our patient P, like in the previously reported patient X-EDA-ID with OL-EDA-ID (Figure 5a). Blood TNF-α production in response to LPS (not shown) or LPS plus IFN-γ (Figure 5b) was also impaired, whereas TNF-α production in response to PMA-ionomycin was less affected. These data indicate that IκBα degradation is a crucial step of the NEMO-dependent NF-κB activation pathway in immune cells stimulated by LPS and IL-1β, as previously shown in patients with complete IRAK-4 deficiency (24). The response of blood cells to TNF-α and IL-18 was not tested.

Although potent stimuli, such as PHA or PMA-ionomycin, were capable of activating naive T cells from our patient in vitro, these cells could not be stimulated by CD3 or recall antigens in vitro and, importantly, did not differentiate into detectable memory T cells in vivo. To further analyze the profound T cell deficiency observed in the IκBα-affected child, we generated T cell blasts by costimulation with PHA and IL-2, and analyzed their phenotype and response to various stimuli. All T cell blasts had normally acquired HLA-DR and CD25 activation markers (not shown) and the CD45RO memory phenotype (Figure 5c), indicating that the lack of blood memory T cells reflected a lack of appropriate antigen-driven TCR-CD3 stimulation in vivo. The memory T cell blasts proliferated and produced IFN-γ perfectly in response not only to PHA and CD3 plus CD28, but also to CD3 alone, indicating that the involvement of IκBα and NF-κB in CD3-mediated T cell activation differs between naive and memory T cells (Figure 5d).

Strikingly, the *NEMO* and *IKBA* mutations are both associated with an impaired response to members of the TIR (TLR, IL-1) and TNFR (EDAR, TNF-αR, and CD40) superfamilies, but the immunodeficiency syndrome associated with IκBα mutation also involves a severe T cell defect, with impaired TCR-CD3–mediated stimulation in vitro. The lack of a T cell response to recall antigens in vitro, together with the lack of detectable memory T cells in peripheral blood despite a marked lymphocytosis, indicates that IκBα degradation is obligatory for TCR-CD3–mediated activation of naive T cells in vivo. The blood T lymphocytosis observed in our patient suggests that T cell homeostasis is also dependent on an intact IκBα degradation. In a related but distinct experimental system, where a gain-of-function IκBα mutant was overexpressed in the T cell lineage by mouse transgenesis, there was also a diminished number of memory CD8 T cells, but in the context of a substantial reduction of the total number of CD8 and to a lesser extent CD4 T cells in the periphery (25–28). No such defects have been observed in *NEMO* patients.

Two hypotheses can be proposed to explain this difference. First, NF-κB is a family of dimeric transcription factors formed by the combination of five distinct subunits (RelA, relB, c-rel, p50, and p52) and the IκB family of proteins may differentially regulate the various NF-κB dimers. NEMO controls the degradation of the three NF-κB inhibitors in various cell types (11–12). Consequently, XL-EDA-ID is associated with similar defects in the degradation of the three IκBs. In contrast, in autosomal dominant EDA-ID, the NF-κB molecules associated with IκBβ and IκBε, but not those associated with IκBα, are normally recruited after IKK activation. The T cell deficiency may therefore result from a disturbed ratio of the various active NF-κB species that reach the T cell nucleus and/or from a decreased mobilization of NF-κB species specifically regulated by IκBα in T cells.

Alternatively, NF-κB activation by TCR-CD3 may not be very sensitive to NEMO mutations because of the existence of alternative, NEMO-independent pathways. Recently, NF-κB–inducing kinase (NIK) has been shown to be involved in T cell activation (29), as well as in several pathways that target IKK1 independently of NEMO (30). Impaired NF-κB activation by CD3 via NIK may thus occur in the IκBα-mutated but not in the NEMO-mutated patients. The inhibition of this NEMO-independent pathway may explain the severe T cell immunodeficiency observed in the IκBα-mutated patient. In any event, our identification of an autosomal dominant form of EDA-ID with severe T cell deficiency expands the spectrum of human diseases caused by defective NF-κB signaling.

Acknowledgments

We thank M. Abinun for helpful discussions and Tatiana Lopez for technical help. This work was supported in part by grants from Ligue Nationale contre le Cancer (équipe labellisée); the Association pour la Recherche sur le Cancer to A. Israël; the Schlumberger Foundation, the BNP-Paribas Foundation, and the EU (QLK2-CT-2002-00846) to J.-L. Casanova; and the Associazione Italiana Ricerca sul Cancro (AIRC) to F. Novelli. J. Reichenbach was supported by the Lise Meitner program.

1. Carrol, E.D., Gennery, A.R., Flood, T.J., Spickett, G.P., Abinun, M. 2003. Anhidrotic ectodermal dysplasia and immunodeficiency: the role of NEMO. *Arch. Dis. Child.* **88**:340–341.
2. Zonana, J., et al. 2000. A novel X-linked disorder of immune deficiency and hypohidrotic ectodermal dysplasia is allelic to incontinentia pigmenti and due to mutations in *IKKγ(NEMO)*. *Am. J. Hum. Genet.* **67**:1555–1562.
3. Döffinger, R., et al. 2001. X-linked anhidrotic ectodermal dysplasia with immunodeficiency is caused by impaired NF-κB signaling. *Nat. Genet.* **27**:277–287.
4. Jain, A., et al. 2001. Specific missense mutations in NEMO result in hyper-IgM syndrome with hypohydrotic ectodermal dysplasia. *Nat. Immunol.* **2**:223–228.
5. Aradhya, S., et al. 2001. Atypical forms of incontinentia pigmenti in male individuals result from mutations of a cytosine tract in exon 10 of NEMO (IKK-γ). *Am. J. Hum. Genet.* **68**:765–771.
6. Mansour, S., et al. 2001. Incontinentia pigmenti in a surviving male is accompanied by hypohidrotic ectodermal dysplasia and recurrent infection. *Am. J. Med. Genet.* **99**:172–177.
7. Dupuis-Girod, S., et al. 2002. Osteopetrosis, lymphedema, anhidrotic ectodermal dysplasia and immunodeficiency in a boy and incontinentia pigmenti in his mother. *Pediatrics.* **109**:e97.
8. Orange, J.S., et al. 2002. Deficient natural killer cell cytotoxicity in patients with IKK-γ/NEMO mutations. *J. Clin. Invest.* **109**:1501–1509. doi:10.1172/JCI200214858.
9. Karin, M., and Ben-Neriah, B. 2002. Phosphorylation meets ubiquitination: the control of NF-κB activity. *Ann. Rev. Immunol.* **18**:621–663.
10. Smahi, A., et al. 2000. Genomic rearrangement in NEMO impairs

NF-κB activation and is a cause of incontinentia pigmenti. *Nature.* **405**:466–472.
11. Courtois, G., Whiteside, S.T., Sibley, C.H., and Israël, A. 1997. Characterization of a mutant cell line that does not activate NF-κB in response to multiple stimuli. *Mol. Cell. Biol.* **17**:1441–1449.
12. Yamaoka, S., et al. 1998. Complementation cloning of NEMO, a component of the IκB kinase complex essential for NF-κB activation. *Cell.* **93**:1231–1240.
13. Whiteside, S.T., et al. 1995. N- and C-terminal sequences control degradation of MAD3/IκBα in response to inducers of NF-κB activity. *Mol. Cell. Biol.* **15**:5339–5345.
14. Rudolph, D., et al. 2000. Severe liver degeneration and lack of NF-κB activation in NEMO/IKKγ-deficient mice. *Genes Dev.* **14**:854–862.
15. Schmidt-Supprian, M., et al. 2000. NEMO/IKKγ-deficient mice model incontinentia pigmenti. *Mol. Cell.* **5**:981–992.
16. Makris, C., et al. 2000. Female mice heterozygous for IKKγ/NEMO deficiencies develop a dermatopathy similar to the human X-linked disorder incontinentia pigmenti. *Mol. Cell.* **5**:969–979.
17. Li, Q., Van Antwerp, D., Mercurio, F., Lee, K.-F., and Verma, I.M. 1999. Severe liver degeneration in mice lacking the IκB kinase 2 gene. *Science.* **284**:321–325.
18. Li, Z.-W., et al. 1999. The IKKβ subunit of IκB kinase (IKK) is essential for NF-κB activation and prevention of apoptosis. *J. Exp. Med.* **189**:1839–1845.
19. Tanaka, M., et al. 1999. Embryonic lethality, liver degeneration, and impaired NF-κB activation in IKK-β-deficient mice. *Immunity.* **10**:421–429.
20. Brockman, J.A., et al. 1995. Coupling of signal response domain in IκB to multiple pathways for NF-κB activation. *Mol. Cell. Biol.* **15**:2809–2818.
21. Brown, K., Gerstberger, S., Carlson, L., Fransozo, G., and Siebenlist, U. 1995. Control of IκBα proteolysis by site-specific, signal-induced phosphorylation. *Science.* **267**:1485–1491.
22. Traenckner, E.B., et al. 1995. Phosphorylation of human IκB on serines 32 and 36 controls IκB proteolysis and NF-κB in response to diverse stimuli. *EMBO J.* **14**:2876–2883.
23. DiDonato, J.A., et al. 1996. Mapping of the inducible IκB phosphorylation sites that signal its ubiquitination and degradation. *Mol. Cell. Biol.* **16**:1295–1304.
24. Picard, C., et al. 2003. Pyogenic bacterial infections in humans with IRAK-4 deficiency. *Science.* **299**:2076–2079.
25. Boothby, M., Mora, A.L., Scherer, D.C., Brockman, J.A., and Ballard, D.W. 1997. Perturbation of the T lymphocyte lineage in transgenic mice expressing a constitutive repressor of nuclear factor (NF)-κB. *J. Exp. Med.* **185**:1897–1907.
26. Esslinger, C.W., Wilson, A., Sordat, B., Beermann, F., and Jongeneel, C.V. 1997. Abnormal T lymphocyte development induced by targeted overexpression of IκBα. *J. Immunol.* **158**:5075–5078.
27. Hettmann, T., DiDonato, J., Karin, M., and Leiden, J. 1999. An essential role for nuclear factor κB in promoting double positive thymocyte apoptosis. *J. Exp. Med.* **189**:145–157.
28. Hettmann, T., Opferman, J.T., Leiden, J.T., and Ashton-Rickardt, P.G. 2002. A critical role for NF-κB transcription factors in the development of $CD8^+$ memory-phenotype cells. *Immunol. Lett.* **85**:297–300.
29. Matsumoto, M., et al. 2002. Essential role of NF-κB-inducing kinase in T cell activation through the TCR/CD3 pathway. *J. Immunol.* **169**:1151–1158.
30. Pomerantz, J.L., and Baltimore, D. 2002. Two pathways to NF-κB. *Mol. Cell.* **10**:693–695.